DOI:
10.1016/j.ifacol.2017.08.1517

Citation for published version (APA):
Yang, X., Sun, J., Lam, H-K., & Dai, J. S. (2017). Fuzzy Model Based Stability Analysis of the Metamorphic Robotic Palm. *IFAC-PapersOnLine*, *50*(1), 8630-8635. https://doi.org/10.1016/j.ifacol.2017.08.1517

Fuzzy Model Based Stability Analysis of the Metamorphic Robotic Palm

Xiaozhan Yang [*] **Jie Sun** [*] **Hak-Keung Lam** [*] **Jian S. Dai** [*]

[*] *Department of Informatics, King's College London, London, WC2R 2LS, United Kingdom (e-mail: xiaozhan.yang@kcl.ac.uk, jie.sun@kcl.ac.uk, hak-keung.lam@kcl.ac.uk, jian.dai@kcl.ac.uk).*

Abstract
Compared with robotic hands with a rigid palm, the metamorphic hand with a reconfigurable palm can alter the palm geometry to relocate the fingers before executing grasping tasks. The stability of dynamics coming with the reconfigurable palm has to be taken into account due to its crucial impact on the performance of the hand. This paper presents the stability analysis of this reconfigurable palm based on its Takagi-Sugeno (T-S) fuzzy model. The dynamic model of the metamorphic palm is developed based on the Euler Lagrangian dynamic theory and the closed-chain kinematic constraints. To reduce the conservativeness in stability analysis and ensure a wider range of stable dynamic performance, a membership-dependent approach is applied to the stability analysis of palm control system. Simulation is provided to demonstrate the achieved improvement of analysis results.

Keywords: Metamorphic palm, dynamic modeling, stability analysis, fuzzy system

1. INTRODUCTION

Grasping and manipulation executed by robotic hands have captured attentions from engineers and researchers with the widespread potential applications of robots in the community. As the end-effector (Cavalieri (1997)) of a robot, a robotic hand is a critical component which can be treated as a robot arm handling the interaction between the robot and the environment. The research on robotic hands has become a thriving subject particularly on designing a robotic hand with the purpose of lowering the cost and achieving some particular standards (Ruiz and Mayol-Cuevas (2016)), for instance, the reliability, repeatability, portability, force capability, etc.

In terms of application fields, robotic hands have two typical categories, grippers and dexterous hands. More specifically, grippers are usually utilized in some industrial applications to perform some pre-programmed tasks, like pick-and-place tasks, with a simple but robust design (Dollar and Howe (2006)). It is unlikely for this type of grippers to perform sophisticated work or complicated manipulation. Its counterpart, the dexterous, high-degree-of-freedom, robotic hands, such as Utah/MIT Hand (Jacobsen et al. (1984)), the NASA Hand (Lovchik and Diftler (1999)), the Shadow Hand (Tuffield and Elias (2003)), etc., are of great dexterity and can generate delicate motion, however, at the expense of high manufacturing and maintaining cost.

As a trade-off of these two design approaches, a metamorphic robotic hand (Dai et al. (2011); Wei et al. (2014); Cui and Dai (2011); Wei et al. (2011)) with a reconfigurable palm was developed through drawing on the advantages of intelligent mechanisms. The palm design was originally inspired by origami with a mechanism equivalent method (Dai and Jones (1999); Dai et al. (2009)) to relate the panels and crisis to links and joints, respectively in such a way to build a flexible robotic palm.

The flexibility of robotic hands can be improved by the reconfigurable palm. At the same time additional dynamics introduced by reconfigurable palm cannot be neglected. Since it is where fingers are mounted, the stability of reconfigurable palm should be crucial for the whole system. As is shown in Fig. 1, the metamorphic palm is a closed-chain mechanism (Ghorbel et al. (2000)) with highly nonlinear kinematic and dynamic relations. Directly stability analysis for the nonlinear palm control system should be not easy, an alternative idea is to describe the system by multi-model methodology (Murray-Smith and Johansen (1997)).

Among the existing multi-model approaches, Takagi-Sugeno (T-S) fuzzy model (Takagi and Sugeno (1985)) is an effective way to investigate the stability problem of highly nonlinear system. It is a model described by fuzzy IF-THEN rules which represents local linear input-output relations of a nonlinear system (Tanaka and Wang (2001)). In this way, the local dynamics can be expressed by a group of local linear models, and the overall fuzzy model can be achieved by fuzzy "blending" of the obtained linear models. As a result, stability analysis of the original nonlinear model can be conducted by the analysis of local linear models.

Motivated by the above discussion, in this paper, we investigate the stability problem of the metamorphic palm control system by the T-S fuzzy model approach. Firstly, dynamic model of the metamorphic palm will be obtained based on the Euler-Lagrange theory and geometric constraints. Then a geometry dependent controller will be applied to compensate the major nonlinearity of model. Finally stability problem will be solved based on the T-S fuzzy model of given closed-loop palm control system.

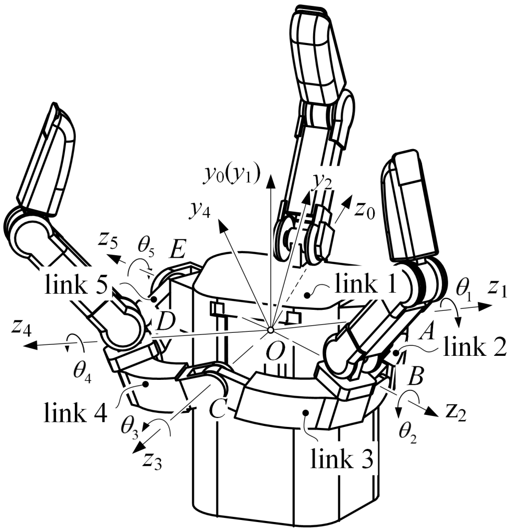

Figure 1. Parameters of the metamorphic hand with a reconfigurable palm

2. DYNAMIC MODELLING OF THE METAMORPHIC PALM BASED ON GEOMETRICAL CONSTRAINTS

The modeling process will be based on the Euler-Lagrangian dynamics. Firstly we need to find the kinetic and potential energy of the metamorphic palm. The palm itself will be divided into two serial chains at joint C, see Fig. 1. The first chain contains links 2 and 3. The second chain contains links 4 and 5. Define the index set as

$$\mathcal{S}_1 \triangleq \{2, 3, 4, 5\}.$$

We introduce the following symbols for the metamorphic palm.

Table 1: Parameter definitions of the metamorphic palm

Symbol	Definition
m_i	The mass of link i ($i \in \mathcal{S}_1$)
I_i^j	The inertia tensor of link i about the center of mass in frame j ($i, j \in \mathcal{S}_1$)
I_i	The inertia tensor of link i about the center of mass in the global frame ($i \in \mathcal{S}_1$)
r_i^j	Position of the center of mass of link i in the body attached frame ($i, j \in \mathcal{S}_1$)
r_i	Position of the center of mass of link i in the global frame ($i \in \mathcal{S}_1$)
v_i	Linear velocity of the center of mass of link i in the global frame ($i \in \mathcal{S}_1$)
ω_i	Angular velocity of the center of mass of link i in the global frame ($i \in \mathcal{S}_1$)
α_i	Arc angle length of link i ($i \in \mathcal{S}_1$)
θ_i	Joint angle from link i to link $i+1$ for $i = 1, 2, 3, 4$, and from link i to link $i-4$ for $i = 5$

Define the skew matrix of a vector $u = [u_x,\ u_y,\ u_z]^T$ as

$$S(u) \triangleq \begin{bmatrix} 0 & -u_z & u_y \\ u_z & 0 & -u_x \\ -u_y & u_x & 0 \end{bmatrix}.$$

Define a rotation matrix for a rotation by an angle of θ about an axis in the direction of u as $R(u, \theta)$, then this matrix can be represented in the following way

$$R(u, \theta) = \cos\theta \cdot I + \sin\theta \cdot S(u) + (1 - \cos\theta) \cdot u \otimes u$$

where $\otimes$ is the tensor product. Also we define unit vectors $\mathbf{i} = [1, 0, 0]^T$, $\mathbf{j} = [0, 1, 0]^T$, $\mathbf{k} = [0, 0, 1]^T$ and following unified vector of joint angles

$$q \triangleq [\,\theta_1\ \theta_5\ \theta_2\ \theta_4\,]^T.$$

Define the rotation from frame i to j as R_i^j, ($i, j \in \mathcal{S}_1$). If a matrix M or vector v depends on q then it will be expressed as $M(q)$ or $v(q)$.

2.1 Kinematics analysis of the partial reconfigurable palm

We start with the open serial chain on the right hand side of the palm. The position of center of mass of link 2 in the global frame should be

$$r_2(q) = R_2^0(q) r_2^2$$

where $R_2^0(q) = R_1^0 R(z_1, \theta_1) R(y_2, -\alpha_2)$ and $R_1^0 = R(y_1, -\frac{1}{2}\alpha_1)$. From (Spong et al. (2006)), linear velocity of center of mass of link 2 in the global frame can be obtained as

$$v_2(q) = S(r_A) r_2(q) \dot{\theta}_1$$

where $r_A = R_1^0 \mathbf{k}$. For the angular velocity, we have

$$\omega_2(q) = r_A \dot{\theta}_1.$$

The position of center of mass of link 3 in the global frame should be

$$r_3(q) = R_2^0(q) R_3^2(q) r_3^3$$

where $R_3^2(q) = R(z_2, \theta_2) R(y_3, -\alpha_3)$. Then the linear velocity of center of mass of link 3 in the global frame is

$$v_3(q) = S(r_A) r_3(q) \dot{\theta}_1 + S(r_B(q)) r_3(q) \dot{\theta}_2$$

where $r_B(q) = R_2^0(q)\mathbf{k}$. Similarly the angular velocity of ω_{3c} can be also obtained in the following way

$$\omega_3(q) = r_A \dot{\theta}_1 + r_B(q) \dot{\theta}_2.$$

By following the same idea, we can have the link kinematic expressions for the left open serial chain. To summarize, we have the following kinematic expressions

$$v_i(q) = J_{v_i}(q)\dot{q}, \quad \omega_i(q) = J_{\omega_i}(q)\dot{q}, \quad \forall\ i \in \mathcal{S}_1$$

where

$$\begin{aligned}
&J_{v_2}(q) = [\,S(r_A) r_2(q)\ 0\ 0\ 0\,], \quad J_{\omega_2}(q) = [\,r_A\ 0\ 0\ 0\,],\\
&J_{v_3}(q) = [\,S(r_A) r_3(q)\ 0\ S(r_B(q)) r_3(q)\ 0\,],\\
&J_{\omega_3}(q) = [\,r_A\ 0\ r_B(q)\ 0\,],\\
&J_{v_4}(q) = [\,0\ -S(r_D(q)) r_4(q)\ 0\ -S(r_E) r_4(q)\,],\\
&J_{\omega_4}(q) = [\,0\ -r_D(q)\ 0\ -r_E\,],\\
&J_{v_5}(q) = [\,0\ 0\ 0\ -S(r_E) r_5(q)\,],\ J_{\omega_5}(q) = [\,0\ 0\ 0\ -r_E\,]
\end{aligned}$$

and

$$\begin{aligned}
&r_E = R_1^0 R(y_1, \alpha_1)\mathbf{k}, \quad r_D = R_5^0(q) R(y_5, \alpha_5)\mathbf{k},\\
&r_5(q) = R_5^0(q) r_5^5, \quad r_4(q) = R_5^0(q) R_4^5(q) r_4^4,\\
&R_5^0(q) = R_1^0 R(y_1, \alpha_1) R(z_5, -\theta_5),\\
&R_4^5(q) = R(y_5, \alpha_5) R(z_4, -\theta_4).
\end{aligned}$$

2.2 Lagrangian method based dynamic modeling of the partial reconfigurable palm

The inertia tensor I_i^i ($i \in \mathcal{S}_1$) of each link expressed in the body attached frame can be obtained by SolidWorks (Planchard and Planchard (2013)) and are constant. To find their expression in the global frame we need the following transformations

$$I_i(q) = R_i^0(q) I_i^i R_i^0(q)^T, \quad (1)$$

for $i \in \mathcal{S}_1$. Overall the kinetic energy should be

$$\mathcal{K}(q) = \frac{1}{2}\dot{q}^T \mathcal{D}(q)\dot{q} \quad (2)$$

where

$$\mathcal{D}(q) = \sum_{i\in\mathcal{S}_1} \left(m_i J_{v_i}(q)^T J_{v_i}(q) + J_{\omega_i}(q)^T I_i(q) J_{\omega_i}(q)\right).$$

The potential energy of all links can be calculated as

$$\mathcal{P}(q) = \sum_{i\in\mathcal{S}_1} m_i g^T r_i(q), \quad i \in \mathcal{S}_1$$

where $g = [0,\ 0,\ 9.81]^T$. Thus from (Ghorbel et al. (2000); Greenwood (1977)), the Euler-Lagrangian dynamic equation can be expressed as

$$\mathcal{D}(q)\ddot{q} + \mathcal{C}(q,\dot{q})\dot{q} + \mathbf{g}(q) = \alpha_q(q)^T\lambda \quad (3)$$

where λ is the vector of Lagrange multipliers, $\alpha_q(q)$ is the parameter obtained from close-chain constraints, $\alpha_q(q)^T\lambda$ represents the constraints generalized force vector. $\mathbf{g}(q)$ is the term related with gravity that can be exactly expressed as

$$\mathbf{g}(q) = \left(\frac{\partial \mathcal{P}(q)}{\partial q}\right)^T = \sum_{i\in\mathcal{S}_1} m_i J_{vi}(q)^T g.$$

And the element on the k-th row and j-column of matrix $\mathcal{C}(q,\dot{q})$ can be represented as

$$c_{kj}(q) = \sum_{i\in\mathcal{S}_1} c_{ijk}(q)\dot{q}_i \quad (4)$$

Define the i-th row and j-th column of matrix $\mathcal{D}(q)$ as $d_{ij}(q)$, then the Christoffel symbol $c_{ijk}(q)$ in (4) can be described as

$$c_{ijk}(q) = \frac{1}{2}\left(\frac{\partial d_{kj}(q)}{\partial q_i} + \frac{\partial d_{ki}(q)}{\partial q_j} - \frac{\partial d_{ij}(q)}{\partial q_k}\right).$$

2.3 Geometrical constraints based palm kinematics analysis

The closed-chain constraints of the palm that the right partial chain and left partial chain are connected at point C is as follows

$$r_{Cr}(q) - r_{Cl}(q) = 0 \quad (5)$$

where $r_{Cr}(q)$ is the position of C calculated from the right serial chain, $r_{Cl}(q)$ is the position of C calculated from the left serial chain, and can be expressed as

$$r_{Cr}(q) = R_2^0(q)R_3^2(q)\mathbf{k}\, r,$$
$$r_{Cl}(q) = R_5^0(q)R_4^5(q)R(y_4,\alpha_4)\mathbf{k}\, r$$

with r being the radius of the palm sphere. In fact, with the physical constraints from the hand wrist, the point C is only allowed to move within the front half sphere of the palm where $z < 0$. Thus we can simply require that $r_{Cr}(q)$ and $r_{Cl}(q)$ have the same projection on the $x-y$ plane. The above constraints can be reduced to

$$\alpha(q) = [I_{2\times2}\ 0_{2\times1}]\cdot(r_{Cr}(q) - r_{Cl}(q)) = 0.$$

The derivatives of $r_{Cl}(q)$ and $r_{Cr}(q)$ with respect to time should be

$$v_{Cr}(q) = S(r_A)r_{Cr}(q)\dot{\theta}_1 + S(r_B(q))r_{Cr}(q)\dot{\theta}_2,$$
$$v_{Cl}(q) = -S(r_E)r_{Cl}(q)\dot{\theta}_5 - S(r_D(q))r_{Cl}(q)\dot{\theta}_4.$$

Calculating the derivative of $\alpha(q)$ with respect to time t, we have

$$\begin{aligned}\alpha_q(q)\dot{q} &= [0_{2\times1}\ I_{2\times2}]\cdot(v_{Cr}(q) - v_{Cl}(q))\\ &= [0_{2\times1}\ I_{2\times2}]\, J_C(q)\dot{q}\end{aligned}$$

where $\alpha_q(q) \triangleq \frac{\partial\alpha(q)}{\partial q}$ and

$$J_C(q) \triangleq \begin{bmatrix} S(r_A)r_{Cr}(q) \\ S(r_E)r_{Cl}(q) \\ S(r_B^0(q))r_{Cr}(q) \\ S(r_D^0(q))r_{Cl}(q)\end{bmatrix}^T.$$

Actually in the palm linkage, the palm structure can be determined by the two active joints θ_1 and θ_2. To reduce the degree of freedom of the model, we define the independent generalized coordinate as

$$p = \beta(q) = \begin{bmatrix} 1\ 0\ 0\ 0 \\ 0\ 1\ 0\ 0\end{bmatrix} q = [I_{2\times2}\ 0_{2\times2}]\, q. \quad (6)$$

Define $\beta_q(q) \triangleq \frac{\partial\beta(q)}{\partial q}$. Obviously it holds that

$$\alpha_q(q) = [I_{2\times2}\ 0_{2\times1}]\, J_C(q), \quad \beta_q(q) = [I_{2\times2}\ 0_{2\times2}].$$

For a specific point in the independent coordinate p, there is a unique mapping point $q = \sigma(p)$ from the dependent coordinate q, among which we define

$$\gamma(q) \triangleq \begin{bmatrix}\alpha(q)\\ \beta(q)\end{bmatrix},\ \gamma_q(q) \triangleq \frac{\partial\gamma(q)}{\partial q},$$

then $\gamma_q(q)$ can be further expressed as

$$\gamma_q(q) \triangleq \begin{bmatrix}\alpha_q(q)\\ \beta_q(q)\end{bmatrix} = \begin{bmatrix}[I_{2\times2}\ 0_{2\times1}]\, J_C(q)\\ [I_{2\times2}\ 0_{2\times2}]\end{bmatrix}$$

From (Ghorbel et al. (2000)) we can get the following mapping relation between $\dot{q}$ and $\dot{p}$,

$$\dot{q} = \rho(q)\dot{p} \quad (7)$$

where

$$\rho(q) = \gamma_q^{-1}(q)\begin{bmatrix}0_{2\times2}\\ I_{2\times2}\end{bmatrix} = \begin{bmatrix} 1 & 0 \\ 0 & 1 \\ \rho_{13}(q) & \rho_{14}(q) \\ \rho_{23}(q) & \rho_{24}(q)\end{bmatrix}.$$

2.4 Dynamic modeling of the reconfigurable palm

The mapping from p to q can be obtained by the spherical cosine law (Wikipedia (2016)). The detailed analysis is presented in the Appendix. Based on the following mapping relations

$$q = \sigma(p), \quad \dot{q} = \rho(q)\dot{p}, \quad (8)$$

we will find the expression of reduced dynamic model in the independent coordinate p. The expression of $\ddot{q}$ can be obtained by taking the derivative of (7),

$$\ddot{q} = \dot{\rho}(q,\dot{q})\dot{p} + \rho(q)\ddot{p}$$

where

$$\dot{\rho}(q,\dot{q}) = \sum_{i=1}^{4}\frac{\partial\rho(q)}{\partial q_i}\dot{q}_i = \sum_{i=1}^{4}\sum_{j=1}^{2}\frac{\partial\rho(q)}{\partial q_i}\rho_{ij}(q)\dot{p}_j.$$

Now the dynamic equation in (3) can be reduced to the following expression of p,

$$\mathsf{D}(p)\ddot{p} + \mathsf{C}(p,\dot{p})\dot{p} + \mathsf{g}(p) = \mathsf{u} \tag{9}$$

with

$$\begin{cases} \mathsf{D}(p) = \rho(q)^T \mathcal{D}(q)\rho(q) \\ \mathsf{C}(p,\dot{p}) = \rho(q)^T \mathcal{C}(q,\dot{q})\rho(q) + \rho(q)^T \mathcal{D}(q)\dot{\rho}(q,\dot{q}) \\ \mathsf{g}(p) = \rho(q)^T \mathbf{g}(q) \end{cases} \tag{10}$$

and

$$\dot{q} = \rho(q)\dot{p}, \quad q = \sigma(p) \tag{11}$$

where the relation of $q = \sigma(p)$ is described in the Appendix.

3. GEOMETRY VARIATION BASED CONTROLLER DESIGN OF THE RECONFIGURABLE PALM

In this part, the control methodology will be based on the following assumption.

Assumption 1. The real-time values of p and $\dot{p}$ can be precisely obtained.

3.1 Controller design method based on inertia and gravity compensation

The control input can be designed as a function of p and $\dot{p}$. Firstly we need the torque to compensate the influence of gravity. Corresponding input would be

$$\mathsf{u}_1(p) = \mathsf{g}(p). \tag{12}$$

The values $\mathsf{g}(p) = [\mathsf{g}_1(p),\ \mathsf{g}_2(p)]^T$ are presented in Fig. 2.

Moreover, additional input $\mathsf{u}_2(p,\dot{p})$ is needed to ensure the system stability and reach the required performance. The relation can be expressed as

$$\mathsf{D}(p)\ddot{p} + \mathsf{C}(p,\dot{p})\dot{p} = \mathsf{u}_2(p,\ \dot{p}) \tag{13}$$

Compared with linear system, the main difference of this dynamic system should be the state-dependent inertial matrix

$$\mathsf{D}(p) = \begin{bmatrix} \mathsf{d}_{11}(p) & \mathsf{d}_{12}(p) \\ \mathsf{d}_{21}(p) & \mathsf{d}_{22}(p) \end{bmatrix}.$$

From (10) we know that $\mathsf{D}(p)$ is symmetric, which means $\mathsf{d}_{21}(p) = \mathsf{d}_{12}(p)$. In Fig. 3, we can find the relation of the elements $\mathsf{d}_{11}(p)$, $\mathsf{d}_{12}(p)$ and $\mathsf{d}_{22}(p)$ of $\mathsf{D}(p)$ with p. In addition, the following relation holds

$$\dot{p}^T \mathsf{D}(p)\dot{p} = \dot{p}^T \rho(q)^T \mathcal{D}(q)\rho(q)\dot{p} = \dot{q}^T \mathcal{D}(q)\dot{q} = 2\mathcal{K}(q)$$

where $\mathcal{K}(q)$ is defined in (2). It means that $\frac{1}{2}\dot{p}^T \mathsf{D}(p)\dot{p}$ is the kinematic energy of the palm, which is generally positive and is zero iff $\dot{p} = 0$. Thus it can be confirmed that $\mathsf{D}(p) > 0$. As a result (13) can be transformed to

$$\ddot{p} + \mathsf{D}(p)^{-1}\mathsf{C}(p,\dot{p})\dot{p} = \mathsf{D}(p)^{-1}\mathsf{u}_2(p,\ \dot{p}) = \bar{\mathsf{u}}_2(p,\ \dot{p}). \tag{14}$$

To analyze the system dynamic performance in the system state space, we define the state as

$$x = [x_1,\ x_2,\ x_3,\ x_4]^T = [\dot{p}_1,\ \dot{p}_2,\ p_1 - p_1^*,\ p_2 - p_2^*]^T$$

where p_1^* and p_2^* are the required positions of θ_1 and θ_5. Equivalently $\bar{\mathsf{u}}_2(p,\ \dot{p})$ can be also expressed as $\bar{\mathsf{u}}_2(x)$.

As it is stated in (Ge et al. (1998)), $\mathsf{C}(p,\dot{p})\dot{p}$ is a combination of *centrifugal forces* and *Coriolis forces*. Both of them depend on the velocity term $\dot{p}$. For the problem of palm position control, the dynamic speed $|\dot{p}|$ is generally low.

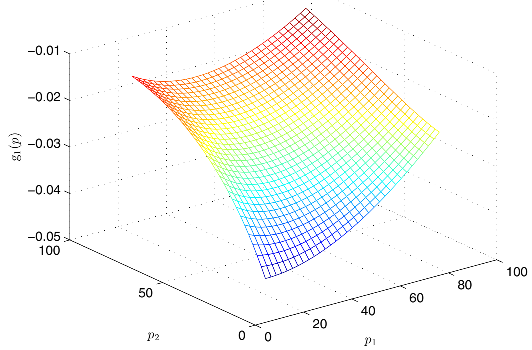

(a) Relation between gravity parameter $\mathsf{g}_1(p)$ and oint state p

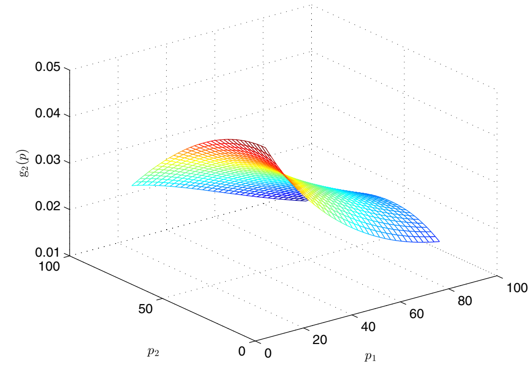

(b) Relation between gravity parameter $\mathsf{g}_2(p)$ and joint state p

Figure 2. Relation between parameters gravity vector $\mathsf{g}(p)$ and joint state p

Also, from (10) we can clearly see that the computation of real-time value of $\mathsf{C}(p,\dot{p})$ is much more complex and time-consuming than that of $\mathsf{D}(p)$. In this sense, we may neglect the influence of $\mathsf{C}(p,\dot{p})\dot{p}$ in the dynamic performance analysis and treat it as the system uncertainty $\Delta\mathsf{A}(x)x$. Then the system equation should be

$$\dot{x} = \mathsf{A}x + \Delta\mathsf{A}(x)x + \mathsf{B}\bar{\mathsf{u}}_2(x) \tag{15}$$

where

$$\mathsf{A} = \begin{bmatrix} 0_{2\times2} & 0_{2\times2} \\ \mathsf{E}_{2\times2} & 0_{2\times2} \end{bmatrix}, \quad \mathsf{B} = \begin{bmatrix} \mathsf{E}_{2\times2} \\ 0_{2\times2} \end{bmatrix},$$

$$\Delta\mathsf{A}(x) = \begin{bmatrix} \mathsf{D}(p)^{-1}\mathsf{C}(p,\dot{p}) & 0_{2\times2} \\ 0_{2\times2} & 0_{2\times2} \end{bmatrix}.$$

Now choose $\bar{\mathsf{u}}_2(x)$ as the linear function of x, which satisfies

$$\bar{\mathsf{u}}_2(x) = \mathsf{K}x = \begin{bmatrix} \mathsf{k}_{11} & 0 & \mathsf{k}_{12} & 0 \\ 0 & \mathsf{k}_{21} & 0 & \mathsf{k}_{22} \end{bmatrix} x.$$

3.2 Dynamic performance analysis

If we neglect the influence of uncertainty $\Delta\mathsf{A}(x)$, the state matrix for closed-loop system should be

$$\hat{\mathsf{A}} = \mathsf{A} + \mathsf{B}\mathsf{K}. \tag{16}$$

The corresponding characteristic equation would be

$$\det(s\mathsf{E} - \hat{\mathsf{A}}) = (s^2 - \mathsf{k}_{11}s - \mathsf{k}_{12})(s^2 - \mathsf{k}_{21}s - \mathsf{k}_{22}). \tag{17}$$

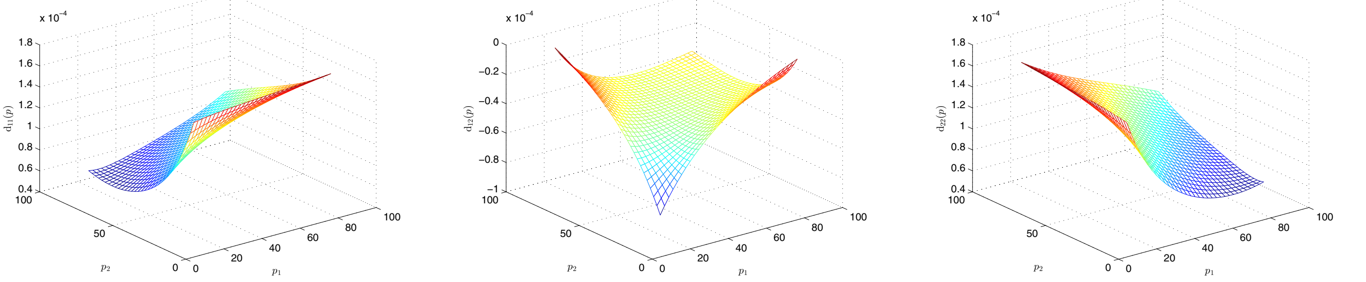

(a) Relation between the inertia parameter $\mathsf{d}_{11}(p)$ and joint state p

(b) Relation between the inertia parameter $\mathsf{d}_{12}(p)$ and joint state p

(c) Relation between the inertia parameter $\mathsf{d}_{22}(p)$ and joint state p

Figure 3. Relation between the parameters in inertia matrix $\mathsf{D}(p)$ and joint state p

The first factor is related with the performance of $\theta_1(t)$, the second factor is related with performance of $\theta_2(t)$. In some sense, this kind of controller can be also regarded as the modified Proportional-Differential (PD) controller. Exactly, k_{11} and k_{12} are the differential and proportional parameters related with $\theta_1(t)$, and k_{21} and k_{22} are the differential and proportional parameters related with θ_2. In this manner, the controllers related with $\theta_1(t)$ and $\theta_2(t)$ have been decoupled from each other and can be designed independently. In this specific case, the palm structure in Fig. 1 is symmetric, thus we can simply choose $\mathsf{k}_{11} = \mathsf{k}_{21} = \mathsf{k}_1$ and $\mathsf{k}_{12} = \mathsf{k}_{22} = \mathsf{k}_2$ to ensure the same dynamic performance of $\theta_1(t)$ and $\theta_2(t)$. Consequently, (17) can be simplified as

$$\det(s\mathsf{E} - \hat{\mathsf{A}}) = (s^2 - \mathsf{k}_1 s - \mathsf{k}_2)^2.$$

4. FUZZY MODEL BASED STABILITY ANALYSIS

In the real case, stability is the basic requirement for any system to work normally, specially for the metamorphic palm, which is the base of fingers. Thus the influence of term $\mathsf{C}(p,\dot{p})\dot{p}$ on system stability cannot be neglected. It means that, within the working space of p and $\dot{p}$, the designed feedback gain K should also ensure the system stability for any $\mathsf{C}(p,\dot{p})\dot{p}$. From (15) and (16), we have

$$\dot{x} = (\hat{\mathsf{A}} + \Delta\mathsf{A}(x))x \tag{18}$$

where

$$\hat{\mathsf{A}} = \begin{bmatrix} \mathsf{k}_1\mathsf{E}_2 & \mathsf{k}_2\mathsf{E}_2 \\ \mathsf{E}_2 & 0_{2\times2} \end{bmatrix}, \quad \Delta\mathsf{A}(x) = \begin{bmatrix} \mathsf{M}(x) & 0_{2\times2} \\ 0_{2\times2} & 0_{2\times2} \end{bmatrix}$$

and

$$\mathsf{M}(x) = \mathsf{D}(p)^{-1}\mathsf{C}(p,\dot{p}) = \begin{bmatrix} \mathsf{m}_{11}(x) & \mathsf{m}_{12}(x) \\ \mathsf{m}_{21}(x) & \mathsf{m}_{22}(x) \end{bmatrix}.$$

Here we consider the stability problem of palm control system in the following task domain $x \in \mathcal{S}$,

$$\mathcal{S} \triangleq \{x|\pi < x_1 < \frac{3\pi}{2}, -\frac{\pi}{2} < x_2 < \pi, |x_3| < 10, |x_4| < 10\}.$$

Generally it is difficult to consider the palm stability problem based on its original nonlinear model in (18). One alternative approach is to replace the state dependent matrix $\Delta\mathsf{A}(x)$ by the combination of finite number of constant matrices. The automatic fuzzy modeling method for nonlinear systems can be found in (Schwaab et al. (2015)). Here, to clearly explain the modeling details, we consider the idea of sector nonlinearity concept (Tanaka and Wang (2001)) to manually find its equivalent T-S fuzzy model. The state-dependent parameters $\mathsf{m}_{ij}(x)$ (the i, j elements of $\mathsf{M}(x)$, $i,j = 1,2$) are all highly nonlinear functions of x_1, x_2, x_3, x_4. For each element $\mathsf{m}_{ij}(x)$ $(i,j = 1,2)$ of $\mathsf{M}(x)$, we can find its maximum and minimum values

$$\mathsf{m}_{ij1} = \max_{x\in\mathcal{S}} \mathsf{m}_{ij}(x), \quad \mathsf{m}_{ij2} = \min_{x\in\mathcal{S}} \mathsf{m}_{ij}(x).$$

Their exact values can be obtained based on the palm technical details in its SolidWorks model.

Table 2: Maximum and minimum values of the parameters $\mathsf{m}_{ij}(x)$, $i,j = 1,2$

	m_{11k}	m_{12k}	m_{21k}	m_{22k}
k = 1	12.86	34.07	26.17	24.80
k = 2	−12.86	−34.07	−26.17	−24.80

The variable $\mathsf{m}_{ij}(x)$ can be expressed as a linear combination of its extrema values, that is

$$\mathsf{m}_{ij}(x) = h_{ij1}(x)\mathsf{m}_{ij1} + h_{ij2}(x)\mathsf{m}_{ij2}$$

where

$$h_{ij1}(x) = \frac{\mathsf{m}_{ij}(x) - \mathsf{m}_{ij2}}{\mathsf{m}_{ij1} - \mathsf{m}_{ij2}}, \quad h_{ij2}(x) = \frac{\mathsf{m}_{ij1} - \mathsf{m}_{ij}(x)}{\mathsf{m}_{ij1} - \mathsf{m}_{ij2}}.$$

In this way, $\mathsf{M}(x)$ can be represented as

$$\mathsf{M}(x) = \sum_{i=1}^{2}\sum_{j=1}^{2}\sum_{k=1}^{2}\sum_{l=1}^{2} h_{11i}(x)h_{12j}(x)h_{21k}(x)h_{22l}(x) \cdot \mathsf{M}_{ijkl}$$

with $\mathsf{M}_{ijkl} = \begin{bmatrix} \mathsf{m}_{11i} & \mathsf{m}_{12j} \\ \mathsf{m}_{21k} & \mathsf{m}_{22l} \end{bmatrix}$. Define the new membership functions and subsystems as

$$\tilde{h}_m(x) \triangleq h_{11i}(x)h_{12j}(x)h_{21k}(x)h_{22l}(x),$$

$$\tilde{\mathsf{A}}_m \triangleq \hat{\mathsf{A}} + \begin{bmatrix} \mathsf{M}_{ijkl} & 0_{2\times2} \\ 0_{2\times2} & 0_{2\times2} \end{bmatrix} \tag{19}$$

with $m = 8i + 4j + 2k + l - 15$ for all $i,j,k,l = 1,2$. It follows that $\hat{\mathsf{A}} + \Delta\mathsf{A}(x) = \sum_{i=1}^{16} \tilde{h}_i(x)\tilde{\mathsf{A}}_i$, and the T-S fuzzy model of (18) becomes

$$\dot{x} = \sum_{i=1}^{16} \tilde{h}_i(x)\tilde{\mathsf{A}}_i x.$$

Now the stability analysis methods (Tanaka and Wang (2001); Yang et al. (2016)) obtained based on T-S fuzzy model can be used to solve the palm stability problem. In the following part we will adopt the stability condition in (Yang et al. (2016)) to reduce the conservativeness of stability analysis. For comparison, we will start with commonly used basic stability condition in (Tanaka and Wang (2001)) which can be expressed as

Lemma 1. (Tanaka and Wang (2001)) If there exists a matrix $P > 0$, such that all the following inequalities hold

$$\tilde{\mathsf{A}}_i^T P + P\tilde{\mathsf{A}}_i < 0, \qquad \forall\, i = 1, 2, \cdots, 16. \tag{20}$$

then system (5) is asymptotically stable.

The palm *stability region* is defined as the range of $(\mathsf{k}_1, \mathsf{k}_2)$ that ensures the stability of palm control system in (18). This region can be estimated by the stability condition in Lemma 1. Changing the values of k_1 and k_2, with the obtained matrices $\tilde{\mathsf{A}}_m$ $(m = 1, 2, \cdots, 16)$, if condition (20) in Lemma 1 is satisfied, then the set $(\mathsf{k}_1, \mathsf{k}_2)$ should be contained in the stability region. In this way, we can find the estimated stability region as

$$\{\mathsf{k}_1, \mathsf{k}_2 \mid \mathsf{k}_1 \le -49.3,\ \mathsf{k}_2 < 0\}. \tag{21}$$

Clearly the basic stability analysis method in Lemma 1 is membership-independent, undoubtedly it should be relatively conservative. To reduce the conservativeness of stability analysis, we adopt the following membership-dependent method in (Yang et al. (2016)).

Theorem 1. (Yang et al. (2016)) If there exists a matrix $P > 0$, such that the following inequality holds

$$\sum_{k=1}^{16} \lambda_{ijk} (\tilde{\mathsf{A}}_k^T P + P\tilde{\mathsf{A}}_k) < 0 \tag{22}$$

for all $i = 1, 2, \cdots, 16$ and $j = 1, 2, \cdots, 15$. Then system (5) is asymptotically stable.

In Theorem 1, λ_{ijk} is a parameter obtained by *Algorithm 1* in (Yang et al. (2016)). With this theorem, the 16 linear matrix inequalities (LMIs) in Lemma 1 will be replaced by 16×15 new LMIs, and conservativeness will be greatly reduced. To get the value of λ_{ijk}, all the maximum and minimum values of $\tilde{h}_i(x)$ $(i = 1, 2, \cdots, 16)$ should be known. Based on the SolidWorks design of this metamorphic palm, one can numerically find the maximum and minimum values of $\tilde{h}_i(x)$ for all $x \in \mathcal{S}$, see Fig. 4. Following the calculation in *Algorithm 1* of (Yang et al. (2016)), we can get the parameters λ_{ijk} for all $i = 1, 2, \cdots, 16$, $j = 1, 2, \cdots, 15$ and $k = 1, 2, \cdots, 16$. By condition (22) in Theorem 1 the estimated stability region of $(\mathsf{k}_1, \mathsf{k}_2)$ can be further improved to

$$\{\mathsf{k}_1, \mathsf{k}_2 \mid \mathsf{k}_1 \le -25.9,\ \mathsf{k}_2 < 0\}. \tag{23}$$

In this way, the feasible range of k_1 and k_2 has been enlarged, and we will get more freedom to tune the dynamic performances.

We set the parameters k_1 and k_2 based on the time-domain dynamic performance criteria in (Hu et al. (2001)). Choose the desired settling time as $t_s = 0.15s$ and overshoot as $\sigma\% = 4.3\%$. By relations in (Hu et al. (2001)), k_1 and k_2 can be obtained as

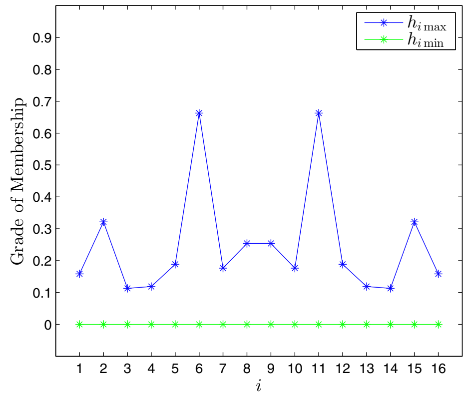

Figure 4. Maximum and minimum values of $h_i(x)$, $i = 1, 2, \cdots, 16$

$$\mathsf{k}_1 = \frac{7}{-t_s} = -46.67,$$
$$\mathsf{k}_2 = -\frac{\mathsf{k}_1^2}{4}\left(\frac{\pi + \ln\sigma\%}{\ln\sigma\%}\right)^2 = -1088.90$$

In the above case, $(\mathsf{k}_1, \mathsf{k}_2)$ is out of region (21) but still contained in (23), which verifies the improvement of method in Theorem 1. By the SimMechanics$^{\text{TM}}$ toolbox, we can get the dynamic simulation of this palm. The angles of active joints at points A and E are plotted in Fig. 5. It is clear that the palm system is still stable, which verifies the less conservativeness of the new stability analysis method.

5. CONCLUSIONS

The dynamic model of the metamorphic palm has been obtained based on the Lagrange-Euler dynamics and the closed-chain geometric constraints. A geometry based controller has been adopted to compensate the model nonlinearity related with the joint positions. By describing the closed-loop system dynamics with a T-S fuzzy model, membership-dependent analysis method has been applied to get the less conservative stability condition. As a result, wider range of control parameters can be used to achieve better dynamic performance.

ACKNOWLEDGEMENTS

The authors gratefully acknowledge the support from King's College London, China Scholarship Council and the European Commission 7th Framework Program SQUIRREL under Grant No. 610532.

Appendix A

A.1 The algorithm to get $q = \sigma(p)$ by spherical cosine law

In this section, we will explain how to get the values of θ_2 and θ_4 from θ_1 and θ_5 based on the closed-chain constraint. The main algorithm will be based on the spherical sine and cosine laws which can be expressed as:

$$\frac{\sin\phi_{AB}}{\sin\psi_{ACB}} = \frac{\sin\phi_{BC}}{\sin\psi_{BAC}} = \frac{\sin\phi_{CA}}{\sin\psi_{CBA}},$$

$$\cos\phi_{AC} = \cos\phi_{AB}\cos\phi_{BC} + \sin\phi_{AB}\sin\phi_{BC}\cos\psi_{ABC}$$

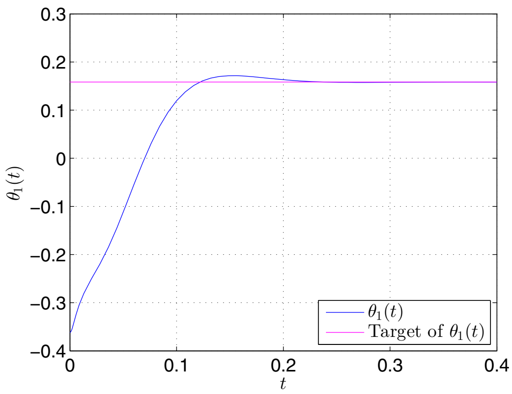

(a) Dynamic trajectory of joint angle $\theta_1(t)$ under the given control parameter k_1 and k_2

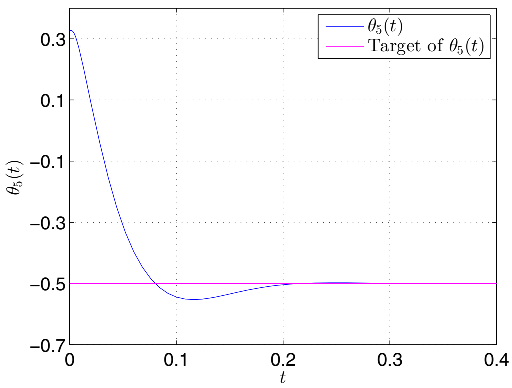

(b) Dynamic trajectory of joint angle $\theta_5(t)$ under the given control parameter k_1 and k_2

Figure 5. Dynamic trajectories of joint angles $\theta_1(t)$ and $\theta_5(t)$ under the given control parameter k_1 and k_2

where ϕ_{AB} means the minor arc between OA and OB measured in degrees with $\phi_{AB} \in [0, \pi)$, and ψ_{ACB} means the spherical angle from ϕ_{CA} to ϕ_{CB} with $\psi_{ACB} \in [-\pi, \pi)$.

It is clear that the following relations hold

$$\phi_{AB} = \alpha_1, \quad \phi_{BC} = \alpha_2, \quad \phi_{CD} = \alpha_3,$$
$$\phi_{DE} = \alpha_4, \quad \phi_{EA} = \alpha_5.$$

For the left hand chain we can find the following relations based on the spherical triangle DEA.

$$\cos\phi_{DA} = \cos\phi_{DE}\cos\phi_{EA} + \sin\phi_{DE}\sin\phi_{EA}\cos\psi_{DEA},$$
$$\cos\phi_{ED} = \cos\phi_{EA}\cos\phi_{AD} + \sin\phi_{EA}\sin\phi_{AD}\cos\psi_{EAD},$$
$$\cos\phi_{AE} = \cos\phi_{AD}\cos\phi_{DE} + \sin\phi_{AD}\sin\phi_{DE}\cos\psi_{ADE}.$$

In the above equations, ϕ_{DE}, ϕ_{EA} and ψ_{DEA} are known angles. What we want are the values of ϕ_{DA}, ψ_{EAD} and ψ_{ADE}. Since ϕ_{DA} is defined as an angle in $[0, \pi)$, we can directly obtain its value by the function $\mathrm{acos}(\cdot)$. But for $\psi_{EAD}, \psi_{ADE} \in [-\pi, \pi)$, we need additional angle ψ_{DEA} to describe the signs of them. Consequently, it follows that

$$\phi_{DA} = \mathrm{acos}(\cos\phi_{DE}\cos\phi_{EA} + \sin\phi_{DE}\sin\phi_{EA}\cos\psi_{DEA}),$$
$$\psi_{EAD} = \mathrm{sign}(\sin\psi_{DEA}) \cdot \mathrm{acos}(\frac{\cos\phi_{ED} - \cos\phi_{EA}\cos\phi_{AD}}{\sin\phi_{EA}\sin\phi_{AD}}),$$
$$\psi_{ADE} = \mathrm{sign}(\sin\psi_{DEA}) \cdot \mathrm{acos}(\frac{\cos\phi_{AE} - \cos\phi_{AD}\cos\phi_{DE}}{\sin\phi_{AD}\sin\phi_{DE}}).$$

Similarly, for the spherical triangle EAB on the right hand serial chain, it holds that

$$\phi_{EB} = \mathrm{acos}(\cos\phi_{EA}\cos\phi_{AB} + \sin\phi_{EA}\sin\phi_{AB}\cos\psi_{EAB}),$$
$$\psi_{ABE} = \mathrm{sign}(\sin\psi_{EAB}) \cdot \mathrm{acos}(\frac{\cos\phi_{AE} - \cos\phi_{AB}\cos\phi_{BE}}{\sin\phi_{AB}\sin\phi_{BE}}),$$
$$\psi_{BEA} = \mathrm{sign}(\sin\psi_{EAB}) \cdot \mathrm{acos}(\frac{\cos\phi_{BA} - \cos\phi_{BE}\cos\phi_{EA}}{\sin\phi_{BE}\sin\phi_{EA}}).$$

From the spherical triangle DAB, we can get the value of ϕ_{DB}, which is

$$\phi_{DB} = \mathrm{acos}(\cos\phi_{DA}\cos\phi_{AB} + \sin\phi_{DA}\sin\phi_{AB}\cos\psi_{DAB}).$$

From the spherical triangle BCD, we have

$$|\psi_{BCD}| = \mathrm{acos}(\frac{\cos\phi_{BD} - \cos\phi_{BC}\cos\phi_{CD}}{\sin\phi_{BC}\sin\phi_{CD}}). \qquad \text{(A.1)}$$

The sign of ψ_{BCD} depends on the working mode of the metamorphic palm. If the palm is working in the lower half sphere, ψ_{BCD} should be positive. Otherwise, it should be negative. Based on the spherical sine law, we can get the other spherical angles in spherical triangle BCD,

$$\psi_{DBC} = \mathrm{asin}(\frac{\sin\psi_{BCD}\sin\phi_{CD}}{\sin\phi_{BD}}),$$
$$\psi_{CDB} = \mathrm{asin}(\frac{\sin\psi_{BCD}\sin\phi_{BC}}{\sin\phi_{BD}}).$$

By spherical triangles EBD and BDA, we can get the following results

$$\psi_{EBD} = \mathrm{sign}(\sin\psi_{DEB}) \cdot \mathrm{acos}(\frac{\cos\phi_{ED} - \cos\phi_{EB}\cos\phi_{BD}}{\sin\phi_{EB}\sin\phi_{BD}}),$$
$$\psi_{BDA} = \mathrm{sign}(\sin\psi_{DAB}) \cdot \mathrm{acos}(\frac{\cos\phi_{BA} - \cos\phi_{BD}\cos\phi_{DA}}{\sin\phi_{BD}\sin\phi_{DA}})$$

where

$$\psi_{DEB} = \psi_{DEA} - \psi_{BEA}, \quad \psi_{DAB} = \psi_{EAB} - \psi_{EAD}.$$

Overall the values of θ_2 and θ_4 can be obtained as

$$\theta_2 = \psi_{ABC} = \psi_{ABE} + \psi_{EBD} + \psi_{DBC},$$
$$\theta_4 = \psi_{CDE} = \psi_{CDB} + \psi_{BDA} + \psi_{ADE}.$$

REFERENCES

Cavalieri, S. (1997). A solution to the end-effector position optimisation problem in robotics using neural networks. *Neural Computing & Applications*, 5(1), 45–57.

Cui, L. and Dai, J.S. (2011). Posture, workspace, and manipulability of the metamorphic multifingered hand with an articulated palm. *Journal of Mechanisms and Robotics*, 3(2), 021001–1–021001–7.

Dai, J.S. and Jones, J.R. (1999). Mobility in metamorphic mechanisms of foldable/erectable kinds. *Journal of Mechanical Design*, 121(3), 375–382.

Dai, J.S., Wang, D., and Cui, L. (2009). Orientation and workspace analysis of the multifingered metamorphic hand–metahand. *IEEE Transactions on Robotics*, 25(4), 942–947.

Dai, J.S., Wei, G., Wang, S., Luo, H., and Li, J. (2011). An anthropomorphic hand with reconfigurable palm.

Dollar, A.M. and Howe, R.D. (2006). Joint coupling design of underactuated grippers. In *ASME 2006 International Design Engineering Technical Conferences and Computers and Information in Engineering Conference*, 903–911. American Society of Mechanical Engineers.

Ge, S.S., Lee, T.H., and Harris, C.J. (1998). *Adaptive Neural Network Control of Robotic Manipulators*. World Scientific, Singapore.

Ghorbel, F.H., Chetelat, O., Gunawardana, R., and Longchamp, R. (2000). Modeling and set point control of closed-chain mechanisms: Theory and experiment. *IEEE Transactions on Control Systems Technology*, 8(5), 801–815.

Greenwood, D.T. (1977). *Classical Dynamics.* Prentice-Hall, Englewood Cliffs.

Hu, S. et al. (2001). *Principles of Automatic Control [in Chinese].* Science Press, Beijing.

Jacobsen, S.C., Wood, J.E., Knutti, D.F., and Biggers, B. (1984). The UTAH/M.I.T. dextrous hand work in progress. *International Journal of Robotics Research*, 3(4), 21–50.

Lovchik, C.S. and Diftler, M.A. (1999). The robonaut hand: a dexterous robot hand for space. In *Proceedings of the 1999 IEEE International Conference on Robotics & Automation.* Detroit, Michigan.

Murray-Smith, R. and Johansen, T.A. (1997). *Multiple Model Approaches to Modelling and Control.* Taylor and Francis, London.

Planchard, D.C. and Planchard, M.P. (2013). *SolidWorks 2013 Tutorial.* SDC Publications.

Ruiz, E. and Mayol-Cuevas, W. (2016). Towards an objective evaluation of underactuated gripper designs. *arXiv preprint arXiv:1601.04547.*

Schwaab, A.A.S., Nassar, S.F., and Filho, P.J.F. (2015). Automatic methods for generation of type-1 and interval type-2 fuzzy membership functions. *Journal of Computer Science*, 11(9), 976–987.

Spong, M.W., Hutchinson, S., and Vidyasagar, M. (2006). *Robot Modeling and Control.* John Wiley & Sons, New York.

Takagi, T. and Sugeno, M. (1985). Fuzzy identification of systems and its applications to modeling and control. *IEEE Transactions on Systems, Man, and Cybernetics*, SMC-15(1).

Tanaka, K. and Wang, H.O. (2001). *Fuzzy Control Systems Design and Analysis.* John Wiley & Sons, New York.

Tuffield, P. and Elias, H. (2003). The shadow robot mimics human actions. *Industrial Robot*, 30(1), 56–60.

Wei, G., Dai, J.S., Wang, S., and Luo, H. (2011). Kinematic analysis and prototype of a metamorphic anthropomorphic hand with a reconfigurable palm. *International Journal of Humanoid Robotics*, 8(3), 459–479.

Wei, G., Gogu, G., Stephan, F., Aminzadeh, A., Wuerdemann, H., Walker, R., et al. (2014). Dexdeb - application of dextrous robotic hands for deboning operation. *Springer Tracts in Advanced Robotics*, 94, 217–235.

Wikipedia (2016). Spherical law of cosines — wikipedia, the free encyclopedia. URL `https://en.wikipedia.org/w/index.php?title=Spherical_law_of_cosines&oldid=743067771`. [Online; accessed 7-October-2016].

Yang, X., Lam, H.K., and Wu, L. (2016). Novel membership-function-dependent stability condition for t-s fuzzy systems. In *Proceedings of 2016 IEEE World Congress on Computational Intelligence (WCCI2016).* Vancouver, Canada.